Ionics (2015) 21:515–523
DOI 10.1007/s11581-014-1173-5

ORIGINAL PAPER

Facile electrostatic coprecipitation of f-SWCNT/Co_3O_4 nanocomposite as supercapacitor material

Abbas Abdolmaleki · Hanif Kazerooni · Mohammad Bagher Gholivand · Hamid Heydari · Afshin Pendashteh

Received: 24 September 2013 / Revised: 18 May 2014 / Accepted: 27 May 2014 / Published online: 8 June 2014

Abstract A facile electrostatic co-precipitation route has been employed to prepare *f-SWCNT/Co_3O_4* nano-composite. The prepared samples have been characterized by X-ray diffraction, Fourier transform infrared spectroscopy, field emission scanning electron microscopy, transmission electron microscopy and BET. Application of the prepared samples has been evaluated as supercapacitor material in 6 M KOH solution using cyclic voltammetry in different potential scan rates, ranging from 5 to 50 mV s^{-1}, and electrochemical impedance spectroscopy (EIS). The specific capacitance of *f-SWCNT/Co_3O_4* has been calculated to be as high as 343 F g^{-1}, much higher than that of obtained for pure Co_3O_4 nanoparticles (77 F g^{-1}). Moreover, the composite material has shown better rate capability (55 % capacitance retention) in various scan rates in comparison with the pure oxide (40 % retention). The composite material also showed excellent cycling performance (92 % capacitance retention) over 5,000 continuous cycles. EIS results show that the composite material benefits form much lower charge transfer resistance, compared with Co_3O_4 nanoparticles.

Keywords Cobalt oxide · Carbon nanotube · Nanostructures · Supercapacitor

A. Abdolmaleki (✉) · M. B. Gholivand · H. Heydari
Faculty of Sciences, Razi University, P.O. Box 671496-7346, Kermanshah, Iran
e-mail: abbas.abdolmaleki@outlook.com

H. Kazerooni
Faculty of Chemical Engineering, Amirkabir University of Technology, Tehran, Iran

A. Pendashteh (✉)
Department of Chemistry, Tarbiat Modraes University, Tehran, Iran
e-mail: a.pendashteh@gmail.com

Introduction

Electrochemical energy storage has attracted great interests all around the world and in the scientific community due to fossil fuel energy depletion and global warming challenges [1, 2]. In this regard, supercapacitors are one of the most efficient energy storage devices due to high power densities, high energy densities, and inherent long cycle life [3, 4]. Recently, huge attention has been paid to develop two kinds of supercapacitors including electrochemical double-layer capacitors (EDLCs) based on carbonaceous materials with a high surface area, and faradaic pseudo-capacitors based on metal oxides or conducting polymers with several oxidation states [5–7]. The faradic pseudo-capacitors possess higher energy densities while the EDLCs benefit from higher power densities. Among different active materials, composite materials utilize the combination of the two charge storage mechanisms, and their formation is highly of interest and importance [8, 9].

Transition metal oxides have been always one of the most interested materials for pseudo-capacitor applications due to their various oxidation states [10–12]. Among them, cobalt oxide has been reported to be a promising electrode material for pseudo-capacitors due to low cost, abundance, and environment benignity [13–15]. However, poor electrical conductivity and difficulty in the penetration of electrolyte into the structure of metal oxides result in limited charge transfer reaction kinetics, and therefore, a relatively low specific capacitance is obtained.

On the other hand, carbonaceous materials are of interest as EDLC electrode materials. Among various kinds of these materials including meso-porous carbon [16], activated carbon [17], carbon fibers [18], carbon nanotube (CNT) [19, 20], and recently developed graphene [21–23], CNT has attracted most of research attempts as the electrode material for EDLCs, due to its unique one-dimensional meso-porous structure,

highly accessible surface area, good electrical conductivity, and high chemical stability. However, the disadvantage of relatively low specific capacitance has restricted the development of CNT-based EDLCs. Hence, employing of CNTs as additives or in composite materials seems to be a promising strategy to develop metal oxide/CNT composite supercapacitors with high power density and high energy density [24–26]. Cobalt oxide composites with various carbonaceous materials have attracted much attention to utilize the synergistic effects and enhance the metal oxide energy storage properties [27]. For example, Zhao et al. have prepared graphene/SWCNT/Co_3O_4 hybrids by directly grown of SWCNTs on the surface of encapsulated Co_3O_4 nanoparticles in graphene layers using CVD technique. The hybrid material showed a high specific capacitance of 325 F g^{-1} at a scan rate of 10 mV s^{-1} [28]. Zhang et al. have prepared flexible electrospun carbon nanofibers embedded with Co_3O_4 hallow nanoparticles and investigated the electrochemical behavior of the composite material. The obtained 3D porous hybrid films showed a high capacitance of 556 F g^{-1} at a current density of 1 A g^{-1}. Moreover, the hybrid material demonstrated an excellent rate capability and cycle stability [29]. In another report, Zhou et al. have synthesized Co_3O_4 composite with multi-walled CNTs via hydrothermal rout and employed it as an integrated anode for lithium ion batteries, revealing a high reversible capacity and excellent cycling stability for the composite material [30]. Therefore, cobalt oxide/CNT composites with highly conductive CNT and highly pseudo-capacitive cobalt oxide are of great interest. However, to the best of our knowledge, there are a few reports on applicability of the cobalt oxides–CNT composites for supercapacitors [31, 32], and facile synthesis of such composites for supercapacitor applications with improved performance is of highly demand and interest.

Herein, a facile electrostatic co-precipitation approach was employed to hybridize functionalized SWCNTs with Co_3O_4 nanoparticles, and application of the obtained composite material was evaluated as supercapacitor electrode material through cyclic voltammetry technique. The improvement of the composite material resulting from combination of EDLC and pseudo-capacitance mechanisms was evaluated by cyclic voltammetry (CV) at various scan rates and EIS measurements.

Experimental

Synthesis of Co_3O_4 nanoparticles

All chemicals were purchased from Merck and used without any purification. In a typical experiment, 0.07 mol of $Co(NO_3)_2 \cdot 3H_2O$ was dissolved and stirred in 50 ml doubly distilled water. Afterward, 0.2 mol urea was added to the solution as fuel, and temperature was set to 70 °C for 12 h to gradually evaporate the solvent. The obtained powder was then calcined at 400 °C for 6 h.

Synthesis of f-SWCNT/Co_3O_4 nano-composite

SWCNTs were functionalized by refluxing treatment in HNO_3 for 4 h (denoted as f-SWCNT). f-SWCNT/Co_3O_4 nano-composite with a mass ratio of 1:2 was synthesized through an electrostatic co-precipitation method (Scheme 1). Typically, 100 ml of Co_3O_4 nano-particles (0.4 mg/ml) was mixed with 100 ml of f-SWCNT dispersed solution (0.2 mg/ml) under sonication. The mixture was maintained untouched for 3 h. The obtained participate was washed with doubly distilled water for several times and dried at 60 °C.

Characterization

Samples were characterized by X-ray powder diffraction (XRD, using a Philips X'pert diffractometer equipped with Cu K_α radiation at 40 kV and 30 mA with a step size of 0.02 $^\circ s^{-1}$) and Fourier transform infrared spectroscopy (FTIR) spectroscopy. Morphology of the samples was investigated by a Philips field-emission scanning electron microscopy (FE-SEM) at 15.0 kV and transmission electron microscopy (TEM) at 150 kV. The measurement software was used to estimate the average size of the obtained particles from SEM micrographs. Zeta-potential measurements of f-SWCNT and Co_3O_4 suspensions were performed using Zeta-sizer (Malvern Instruments Ltd, England). The pH of the dispersed solutions was adjusted by 0.1 M NaOH and 0.1 M HCl solutions. The surface properties of the samples were characterized by nitrogen adsorption/desorption measurements using a Quantachrome instrument (NOVA station). The electrical conductivity of the samples was also measured by a four-probe method.

Electrochemical measurements

BioLogic Science instrument was employed to evaluate the electrochemical properties of the samples in 6 M KOH solution as the electrolyte in a three-electrode configuration using CV and electrochemical impedance spectroscopy (EIS) techniques. The active material, carbon black, and polyvinylidene fluoride (PVDF) were mixed with a mass ratio of 75:15:10. The mixture was dispersed in a small amount of acetone, and the obtained slurry was pressed on nickel foam and dried at 100 °C. The mass loading of the active material for each electrode was about 1 mg. A SCE electrode and Pt plate were used as the reference and counter electrodes, respectively.

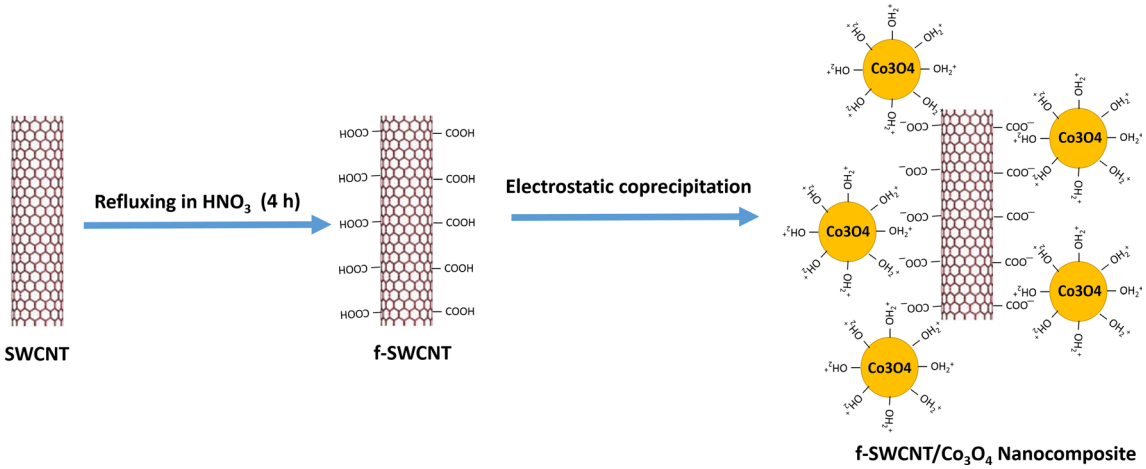

Scheme 1 Electrostatic co-precipitation of f-SWCNT with Co_3O_4 nanoparticles

Results and discussion

Characterization

The electrostatic interaction governing the fabrication of f-SWCNT and Co_3O_4 nanoparticles has been investigated by varying pH of the solutions. Figure 1 shows the zeta-potential profiles of surface charges of f-SWCNT and Co_3O_4 nanoparticles as a function of pH. As it is seen, in most of the measured pH range, f-SWCNT was negatively charged due to the ionization of its functional groups. In contrast, investigation of zeta potential of Co_3O_4 suspension in almost the same pH range revealed that the oxide surface is positively charged in most of the studied range. Accordingly, the most potential gradient is at pH=5, and therefore, this pH was selected for hybridization.

XRD was employed to structurally characterize the samples. Figure 2a shows XRD pattern of the synthesized Co_3O_4 nanoparticles. As it has been marked by *hkl* planes, all of the diffracted peaks can be well assigned to the cubic Co_3O_4 with lattice parameters of a=b=c=8.065 Å (JCPDS-01-074-1657). Moreover, no diffraction lines corresponding to any impurity were detected. As it can be seen from Fig. 2b, f-SWCNT/Co_3O_4 sample includes all of the lines corresponding to the Co_3O_4 crystal except the broad line at 2θ=26° which corresponds to the (0 0 2) reflection of SWCNTs.

FTIR spectroscopy was conducted for further characterization of the samples (Fig. 3). As it can be seen, the f-SWCNT sample includes distinguished peaks at 1,120, 1,578, 1,635, 2,995, and 3,439 cm^{-1} which can be attributed to the C−O, C=C, C=O, carboxylic O−H, and alcoholic O−H bonds, respectively, in chemical modified nanotubes. All of these peaks were also appeared in f-SWCNT/Co_3O_4 sample as well as peaks identified at 587 and 680 cm^{-1} corresponding to the vibrational modes of Co−O bond and confirms the hybridization of Co_3O_4 nano-crystals with f-SWCNT.

The morphology of Co_3O_4 nanoparticles and f-SWCNT/Co_3O_4 nano-composite was investigated using field emission scanning electron microscopy (FESEM). As is seen from Fig. 4a, the Co_3O_4 sample is comprised of cauliflower-like structures which themselves are composed of nanoparticles with particle size in the range of 15–40 nm. Figure 4b shows the FESEM micrograph of the composite material, revealing that the nanoparticles are well dispersed on the surface of SWCNTs. Well-dispersion of the metal oxide on nanotubes will play a key role to form a three-dimensional electronic network and improve the electrical conductivity of the composite material, in comparison with the low relative electrical conductivity of Co_3O_4. The EDX analysis was shown in inset, revealing that the sample comprises of the expected elements of C, Co, and O. Moreover, according to the EDX analysis, carbon content occupies around 35.6 % which is almost the

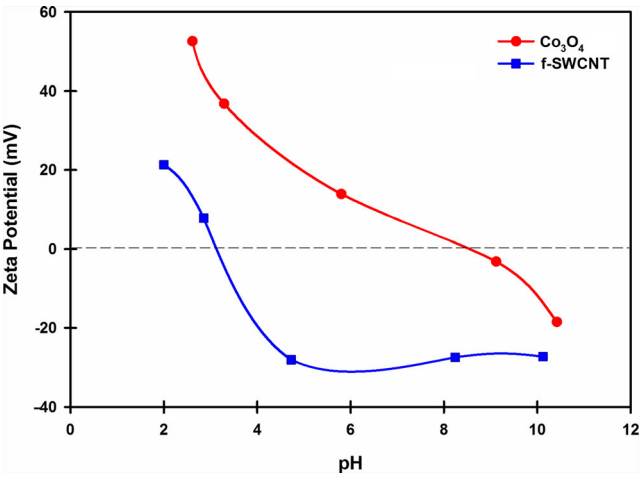

Fig. 1 Zeta-potential profiles of Co_3O_4 and f-SWCNT suspensions in various pH values

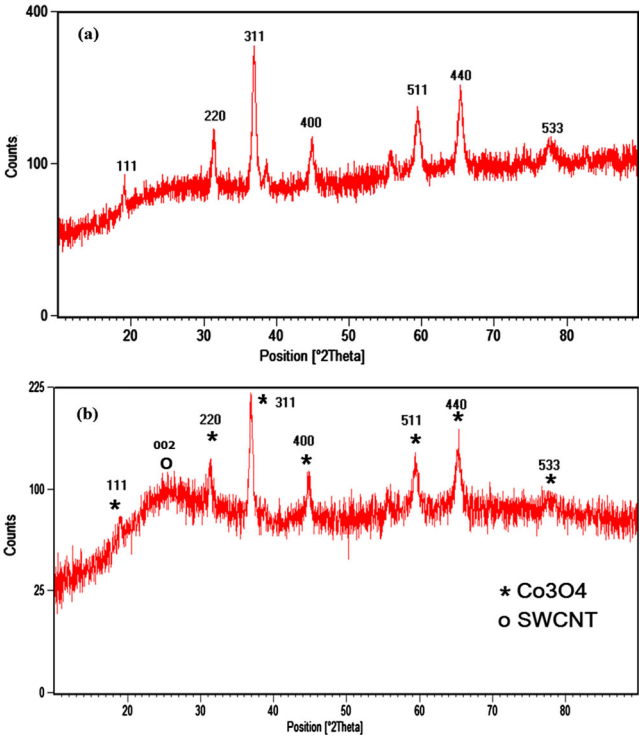

Fig. 2 XRD patterns of Co_3O_4 nanoparticles (**a**), and f-SWCNT/Co_3O_4 nano-composite (**b**)

same amount as used during the synthesis. Figure 4, c and d, shows the TEM images of the composite materials in two different magnifications. As it is clearly seen in Fig. 4d, the Co_3O_4 nanoparticles with a size about 50–70 nm are tightly attached to the carbon nanotubes. Moreover, it can be seen that the Co_3O_4 nanoparticles are themselves comprised of much smaller particles which is in agreement with the cauliflower-like structure seen in the SEM images.

Nitrogen adsorption/desorption isotherms were employed to characterize the surface properties and pore structure of the samples. Figure 5 shows the adsorption/desorption isotherms of the samples. Based on the results from BET calculations, a high specific surface area of 616.32 $m^2\ g^{-1}$ was obtained for the f-SWCNT/Co_3O_4 sample, which is about 3,300 % higher than that of the pure Co_3O_4 sample (18.50 $m^2\ g^{-1}$). This extremely improved specific surface area will results in enhanced access of the electrolyte ions and therefore facilitates the ion diffusion during the charge/discharge process. Moreover, the pore diameter of 2.41 nm was obtained for the composite material according to the BJH method. The surface properties of the samples are provided in the Table 1.

In order to evaluate the electrical conductivity of the samples, a four-probe technique was employed. Based on the results, conductivity of the pure Co_3O_4 sample was obtained as 7.9×10^{-5} S cm^{-1}. This is while that the conductivity value of the composite material was achieved as 3.0×10^{-4} S cm^{-1}. From this finding, it can be clearly understood that the incorporation of the highly conductive SWCNT into the composite sample results in enhanced electrical conductivity of this sample which will facilitate the electron transfer during the electrochemical reactions.

Electrochemical measurements

Cyclic voltammetry (CV) was performed to investigate supercapacitive performance of the synthesized samples. Figure 6a and b shows voltammograms of Co_3O_4 nanoparticles and f-SWCNT/Co_3O_4 nano-composite in 6 M KOH solution as the electrolyte at various scan rates of 5–50 mV s^{-1}. As it is clearly seen, CV curve for the Co_3O_4

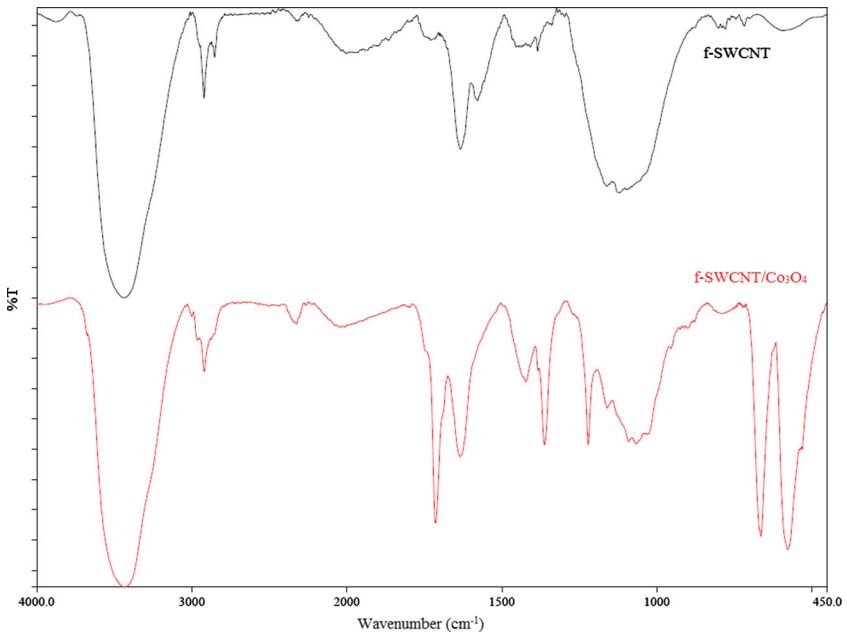

Fig. 3 FTIR spectra of f-SWCNT and f-SWCNT/Co_3O_4 samples

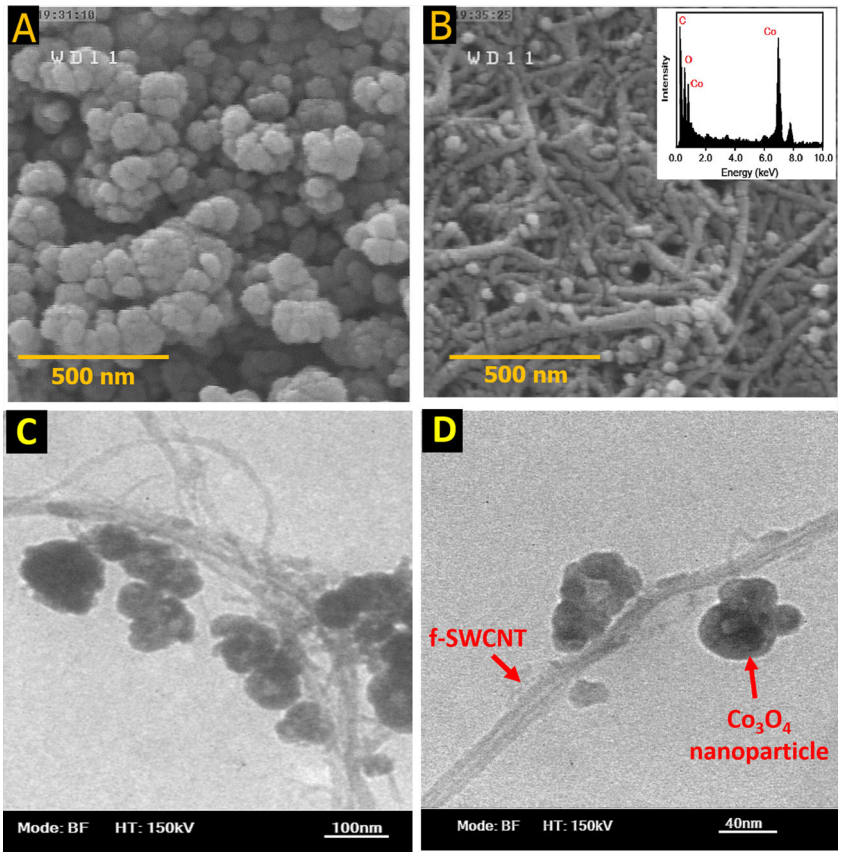

Fig. 4 FESEM micrographs of Co_3O_4 nanoparticles (**a**), f-SWCNT/Co_3O_4 nano-composite (**b**) and TEM images of the composite material (**c** and **d**)

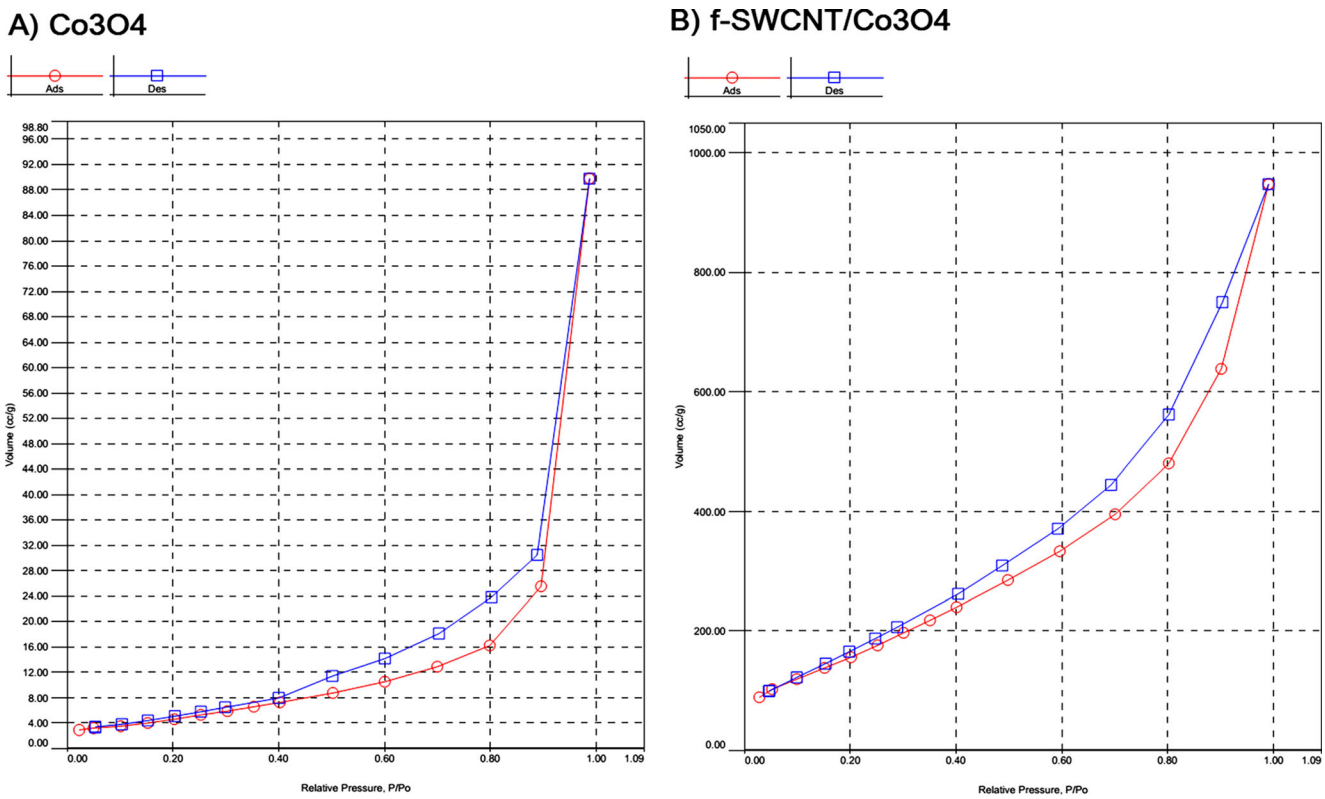

Fig. 5 N_2 adsorption/desorption isotherms of the samples: Co_3O_4 (**a**) and f-SWCNT/Co_3O_4 (**b**)

Table 1 Surface properties and pore structure of the samples

Sample	Surface area ($m^2\ g^{-1}$)[a]	Pore volume (cc g^{-1})[b]	Pore diameter (nm)[b]
Co_3O_4	18.50	0.146	3.643
f-SWCNT/Co_3O_4	616.32	1.60	2.414

[a] Calculation based on BET

[b] Calculation based on BJH

sample is comprised of a distinct pair of redox peaks during the anodic and cathodic sweeps. The redox peaks can be attributed to the conversion between different cobalt oxidation states (Co^{2+}/Co^{3+}; Co^{3+}/Co^{4+}) based on the following equations (Eq. 2):

$$Co_3O_4 + OH^- + H_2O \leftrightarrow 3CoOOH + e^- \quad (1)$$

$$CoOOH + OH^- \leftrightarrow CoO_2 + H_2O + e^- \quad (2)$$

The specific capacitance of the active material can be calculated from the charge transferred through the forward and backward scans. Therefore, it can be calculated using the following equation, Eq. 3:

$$C_{sp} = \frac{\bar{I}}{mv} \quad (3)$$

where C_{sp} is the specific capacitance in Farad per gram, $\bar{I}$ is the average current in amperes, m is the mass of active material in g, and ν is the potential scan rate in volts per second. Hence, the specific capacitance of 77 F g^{-1} was

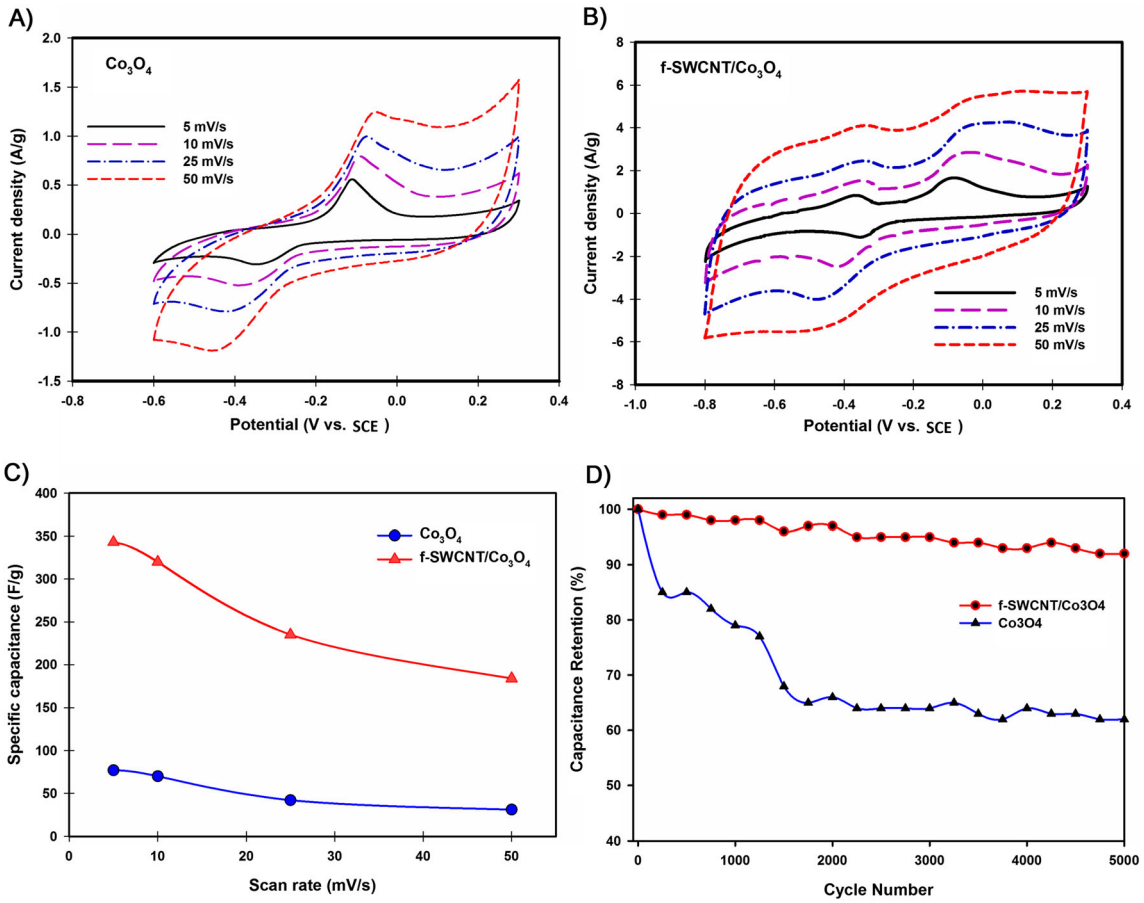

Fig. 6 Cyclic voltammograms for Co_3O_4 nanoparticles (**a**) and f-SWCNT/Co_3O_4 nano-composite (**b**) in 6 M KOH solution as the electrolyte at various scan rates of 5–50 mV s^{-1}. Rate capability of the samples at various scan rates (**c**), and cycling stability of the samples at 25 mV s^{-1} (**d**)

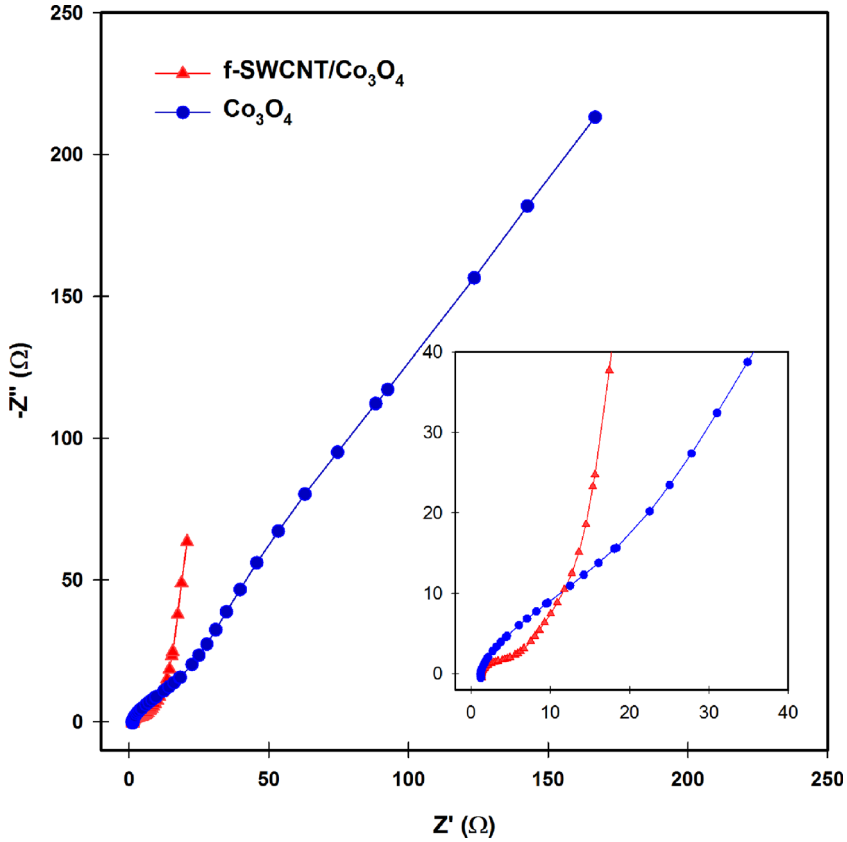

Fig. 7 Nyquist plot for Co_3O_4 nano-particles and f-SWCNT/Co_3O_4 nano-composite electrodes

obtained for Co_3O_4 nanoparticles at the scan rate of 5 mV s^{-1}. Cyclic voltammogram of f-SWCNT/Co_3O_4 includes the same peaks and some more which may be attributed to the functional groups of the SWCNTs. As it is seen from CV, the current densities in composite material have been remarkably increased, in comparison with the Co_3O_4 sample which will result in more charge stored during the charge discharge cycles. The specific capacitance of f-SWCNT/Co_3O_4 composite was calculated through Eq. 1 and found to be 343 F g^{-1} at the scan rate of 5 mV s^{-1}. Moreover, CV curve of the composite material is more close to the relatively rectangle shape which is characteristic of an ideal supercapacitor. All of these findings suggest that dispersion of Co_3O_4 nanoparticles into the SWCNT network can introduce new paths for electron transfer and therefore improve the conductivity and capacitance behavior of the electrodes. The rate performance of the samples was evaluated by comparing the specific capacitances at different scan rates, and the results were shown in Fig. 6c. It is clearly seen that the specific capacitance gradually decreased with the increase of the scan rate. In other words, the specific capacitance was inversely proportional to the scan rate of the measurement. Accordingly, under a relatively high scan rate of 50 mV s^{-1}, nearly 40 % and 55 % of the initial value was remained for pure Co_3O_4, and f-SWCNT/Co_3O_4 electrode, respectively.

In order to investigate cycling performance of the samples, the cycling measurements were conducted up to 5,000 cycles at a scan rate of 25 mV s^{-1} (Fig. 6d). As it is seen, 92 % of the initial capacitance was retained in the composite material, which is much higher than that of the pure Co_3O_4 electrode (about 64 % capacitance retention). The sever capacitance fade in the pure Co_3O_4 electrode is probably due to agglomeration of the nanoparticles during continuous cycling. Incorporating the robust mechanical SWCNT network in the composite material results in significant mechanical stability of the sample and prevents the agglomeration of the metal oxide nanoparticles. Therefore, the obtained results demonstrated good cycling stability of the f-SWCNT/Co_3O_4 composite as supercapacitor electrode material.

For more investigation of the synthesized samples, AC impedance measurements were performed, and the Nyquist plots were shown in Fig. 7. It is seen that both impedance spectra were almost similar, composed of one semicircle component at high-frequency and followed by a linear component at the low-frequency. The semicircle at high-frequency range corresponds to the charge transfer resistance and is clearly smaller in the composite material against pure Co_3O_4. It can be seen that the straight line of the composite material is more vertical which is more closely to an ideal capacitor. All

in all, the composite material showed much better supercapacitive performance compared to the pure metal oxide electrode.

Conclusion

In summary, Co_3O_4 nanoparticles were synthesized by solution combustion method. The as-prepared nanoparticles were used to prepare f-SWCNT/Co_3O_4 nano-composite through a facile electrostatic co-precipitation method. The prepared samples were investigated as supercapacitor electrode materials in 6 M KOH as the electrolyte solution using cyclic voltammetry measurements at various scan rates and electrochemical impedance spectroscopy. Based on the obtained results, the composite material showed much better performance in comparison with pure Co_3O_4 nanoparticles, in terms of specific capacitance (343 F g^{-1} for f-SWCNT/Co_3O_4 compared with 77 F g^{-1} for pure Co_3O_4 at the scan rate of 5 mV s^{-1}) and rate capability. The improvement can be primarily attributed to the combination of the carbonaceous material and metal oxide, as well as the resulted synergistic effect.

References

1. El-Kady MF, Strong V, Dubin S, Kaner RB (2012) Laser scribing of high-performance and flexible graphene-based electrochemical capacitors. Science 335(6074):1326–1330. doi:10.1126/science.1216744
2. Winter M, Brodd RJ (2004) What are batteries, fuel cells, and supercapacitors? Chem Rev 104(10):4245–4270. doi:10.1021/cr020730k
3. Gao W, Singh N, Song L, Liu Z, Reddy ALM, Ci L, Vajtai R, Zhang Q, Wei B, Ajayan PM (2011) Direct laser writing of micro-supercapacitors on hydrated graphite oxide films. Nat Nanotechnol 6(8):496–500. doi:10.1038/nnano.2011.110
4. El-Kady MF, Kaner RB (2013) Scalable fabrication of high-power graphene micro-supercapacitors for flexible and on-chip energy storage. Nat Commun 4:1475. doi:10.1038/ncomms2446
5. Liu C, Yu Z, Neff D, Zhamu A, Jang BZ (2010) Graphene-based supercapacitor with an ultrahigh energy density. Nano Lett 10(12):4863–4868. doi:10.1021/nl102661q
6. Stoller MD, Park S, Zhu Y, An J, Ruoff RS (2008) Graphene-based ultracapacitors. Nano Lett 8(10):3498–3502. doi:10.1021/nl802558y
7. Wu ZS, Zhou G, Yin LC, Ren W, Li F, Cheng HM (2012) Graphene/metal oxide composite electrode materials for energy storage. Nano Energy 1(1):107–131. doi:10.1016/j.nanoen.2011.11.001
8. Kim J-Y, Kim K-H, Yoon S-B, Kim H-K, Park SH, Kim KB (2013) In-situ chemical synthesis of ruthenium oxide/reduced graphene oxide nanocomposites for electrochemical capacitor applications. Nanoscale DOI:. doi:10.1039/C3NR01233F
9. He G, Li J, Chen H, Shi J, Sun X, Chen S, Wang X (2012) Hydrothermal preparation of Co3O4@graphene nanocomposite for supercapacitor with enhanced capacitive performance. Mater Lett 82:61–63. doi:10.1016/j.matlet.2012.05.048
10. Wang G, Huang J, Chen S, Gao Y, Cao D (2011) Preparation and supercapacitance of CuO nanosheet arrays grown on nickel foam. J Power Sources 196(13):5756–5760. doi:10.1016/j.jpowsour.2011.02.049
11. Yu L, Zhang G, Yuan C, Lou XW (2013) Hierarchical NiCo2O4@MnO2 core-shell heterostructured nanowire arrays on Ni foam as high-performance supercapacitor electrodes. Chem Commun 49(2):137–139. doi:10.1039/C2CC37117K
12. Zhang G, Lou XW (2013) General solution growth of mesoporous NiCo2O4 nanosheets on various conductive substrates as high-performance electrodes for supercapacitors. Adv Mater 25(7):976–979. doi:10.1002/adma.201204128
13. Tummala R, Guduru RK, Mohanty PS (2012) Nanostructured Co3O4 electrodes for supercapacitor applications from plasma spray technique. J Power Sources 209:44–51. doi:10.1016/j.jpowsour.2012.02.071
14. Wang H, Zhang L, Tan X, Holt CMB, Zahiri B, Olsen BC, Mitlin D (2011) Supercapacitive properties of hydrothermally synthesized Co3O4 nanostructures. J Phys Chem C 115(35):17599–17605. doi:10.1021/jp2049684
15. Wang G, Shen X, Horvat J, Wang B, Liu H, Wexler D, Yao J (2009) Hydrothermal synthesis and optical, magnetic, and supercapacitance properties of nanoporous cobalt oxide nanorods. J Phys Chem C 113(11):4357–4361. doi:10.1021/jp8106149
16. Hsieh C-T, Hsu S-M, Lin J-Y, Teng H (2011) Electrochemical capacitors based on graphene oxide sheets using different aqueous electrolytes. J Phys Chem C 115(25):12367–12374. doi:10.1021/jp2032687
17. Hulicova-Jurcakova D, Seredych M, Lu GQ, Bandosz TJ (2009) Combined effect of nitrogen- and oxygen-containing functional groups of microporous activated carbon on its electrochemical performance in supercapacitors. Adv Funct Mater 19(3):438–447. doi:10.1002/adfm.200801236
18. McDonough JR, Choi JW, Yang Y, La Mantia F, Zhang Y, Cui Y (2009) Carbon nanofiber supercapacitors with large areal capacitances. Appl Phys Lett 95(24):243109. doi:10.1063/1.3273864
19. Li X, Rong J, Wei B (2010) Electrochemical behavior of single-walled carbon nanotube supercapacitors under compressive stress. ACS Nano 4(10):6039–6049. doi:10.1021/nn101595y
20. Davies A, Yu A (2011) Material advancements in supercapacitors: from activated carbon to carbon nanotube and graphene. Can J Chem Eng 89(6):1342–1357. doi:10.1002/cjce.20586
21. Zhang LL, Zhao S, Tian XN, Zhao XS (2010) Layered graphene oxide nanostructures with sandwiched conducting polymers as supercapacitor electrodes. Langmuir 26(22):17624–17628. doi:10.1021/la103413s
22. Wang Y, Shi Z, Huang Y, Ma Y, Wang C, Chen M, Chen Y (2009) Supercapacitor devices based on graphene materials. J Phys Chem C 113(30):13103–13107. doi:10.1021/jp902214f
23. Mishra AK, Ramaprabhu S (2011) Functionalized graphene-based nanocomposites for supercapacitor application. J Phys Chem C 115(29):14006–14013. doi:10.1021/jp201673e
24. Liu X, Huber TA, Kopac MC, Pickup PG (2009) Ru oxide/carbon nanotube composites for supercapacitors prepared by spontaneous reduction of Ru(VI) and Ru(VII). Electrochim Acta 54(27):7141–7147. doi:10.1016/j.electacta.2009.07.044
25. Ko JM, Kim KM (2009) Electrochemical properties of MnO2/activated carbon nanotube composite as an electrode material for supercapacitor. Mater Chem Phys 114(2–3):837–841. doi:10.1016/j.matchemphys.2008.10.047
26. Yuan C, Xiong S, Zhang X, Shen L, Zhang F, Gao B, Su L (2009) Template-free synthesis of ordered mesoporous NiO/poly(sodium-4-

styrene sulfonate) functionalized carbon nanotubes composite for electrochemical capacitors. Nano Res 2(9):722–732. doi:10.1007/s12274-009-9079-7

27. Wang F, Xiao S, Hou Y, Hu C, Liu L, Wu Y (2013) Electrode materials for aqueous asymmetric supercapacitors. RSC Advances 3:13059–13084. doi:10.1039/C3RA23466E
28. Zhao MQ, Zhang Q, Huang JQ, Tian GL, Chen TC, Qian WZ, Wei F (2013) Towards high purity graphene/single-walled carbon nanotube hybrids with improved electrochemical capacitive performance. Carbon 54:403–411. doi:10.1016/j.carbon.2012.11.055
29. Zhang F, Yuan C, Zhu J, Wang J, Zhang X, Lou XW (2013) Flexible films derived from electrospun carbon nanofibers incorporated with Co_3O_4 hollow nanoparticles as self-supported electrodes for electrochemical capacitors. Adv Func Mater 23:3909–3915. doi:10.1002/adfm.201203844
30. Zhou G, Li L, Zhang Q, Lia N, LI F (2013) Octahedral Co3O4 particles threaded by carbon nanotube arrays as integrated structure anodes for lithium ion batteries. Phys Chem Chem Phys 15:5582–5587. doi:10.1039/C3CP50221J
31. Shan Y, Gao L (2007) Formation and characterization of multi-walled carbon nanotubes/Co3O4 nanocomposites for supercapacitors. Mater Chem Phys 103(2–3):206–210. doi:10.1016/j.matchemphys.2007.02.038
32. Lang J, Yan X, Xue Q (2011) Facile preparation and electrochemical characterization of cobalt oxide/multi-walled carbon nanotube composites for supercapacitors. J Power Sources 196(18):7841–7846. doi:10.1016/j.jpowsour.2011.04.010